Hydrochemical evolution and environmental features of Salso River catchment, central Sicily (Italy)

R. Favara · F. Grassa · M. Valenza

Abstract A hydrogeochemical study of the Salso River highlighted the chemical and isotopic space-time evolution along its flow path and the main contamination processes. Within the basin, three different hydrogeochemical facies have been individuated: (1) Ca-Mg-HCO_3, (2) Ca-Mg-SO_4 and (3) Na-Cl. The first facies reflects the chemical composition of the groundwaters hosted in the carbonate reliefs that belong to the Madonie Mountains. The second and the third facies are the result of the interaction processes between surface waters and the gypsum and salty clays, respectively. Two pollution sources have been also located in the basin downstream from the salt mine and downstream from a discharge area of wastewater from the town of Gangi. On the basis of the location of natural and anthropogenic pollution sources, the waters available for drinking and irrigation use are also indicated.

Key words Geochemistry · Surface and groundwaters water quality

Introduction

The Salso River is located south of the Madonie Mountains, in central Sicily, Italy (Fig. 1). The northern boundary of the studied basin is composed of Madonie carbonate reliefs, whereas the Ponte 5 Archi is the southern boundary. The Madonie reliefs represent one of the largest aquifers in Sicily because of high permeability and the capability to form reservoirs.

Received: 16 July 1999 · Accepted: 22 December 1999

R. Favara (✉)
Istituto di Geochimica dei Fluidi C.N.R., Via Ugo La Malfa, 153, 90146 Palermo, Italy

F. Grassa, M. Valenza
Dipartimento CFTA, Università di Palermo, Via Archirafi 36, 90123 Palermo, Italy

The Salso River has many tributaries, the most important are the southern Imera River and Gangi River. The chemical composition of surface waters is changed by different geochemical processes.
The aims of this study were to determine the interaction processes between rock and water, to individuate the geochemical facies and to define water quality by evaluating the level of pollution inside the Salso River basin. Pollution sources include municipal wastewaters, intense use of fertilisers and pesticides in agriculture, quarry waste and an interaction with highly soluble rocks. These all alter water quality, thus making the water unusable for drinking and/or irrigation use.

Geological framework

The northern boundary of the Salso basin is composed of Madonie carbonate reliefs, which are the source areas for the local groundwater.
The Madonie Mountains are made up of a basic complex that is Upper Triassic-Oligocene in age (Grasso and others 1978), characterized by a marly-calcareous succession on which, tectonically, lies a dolomitic-calcareous succession of 'Falda Panormide' (Cretaceous-Lower Miocene).
The Numidian Flysch (Oligocene-Lower Miocene), made up of thick alternating clay-quartz-sandstone layers, overlies the above successions.
The central part of the basin is composed of sediments that belong to the 'Falda Sicilide', with typical *varicolored* clays (Upper Cretaceous-Lower Miocene), and the Tortonian transitional-facies sediments of the Terravecchia Formation (Lower Miocene).
The remaining central-southern area of the basin is composed of deposits of the 'Gessoso-Solfifera' series (Messinian in age) made up mainly of halite and gypsum.
From a tectonic point of view (Catalano and D'Argenio 1982), from Oligocene to Pleistocene, the study area was involved in alternating compressive and distensive phases, which determined the actual structural setting.

Hydrogeological setting

From a hydrogeological viewpoint, the outcropping rocks may be subdivided into three groups, according to permeability, as follows:

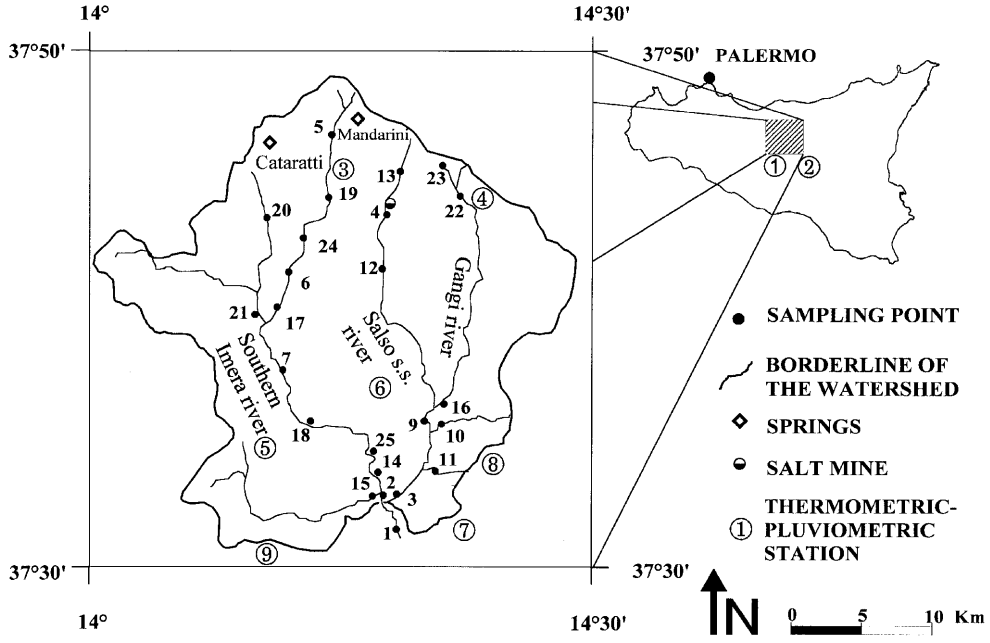

Fig. 1
Location map of the study area. The sampling points and salt mine are shown. The *numbers within the circle* indicate the location of the thermometric (T) and pluviometric (P) station: *1* Caltanissetta (T); *2* Enna (T); *3* Petralia (T and P); *4* Gangi (P); *5* Resuttano (P); *6* Alimena (P); *7* Villadoro (P); *8* Villapriolo (P); *9* S. Caterina Villarmosa (P)

1. Highly permeable
   - Limestone and dolomite that belong to the Panormide domain: they are subject to extreme weathering, enhanced by the very high degree of fracturing. Surface run-off is increased by the steep slope of the reliefs
   - Deposits of the Messinian Gypsum-Solfifera series, which are mainly composed of basic limestone, gypsum and extremely soluble chloride and sulphate salts. In these lithotypes, permeability is high because of both fracturing and the effects of karst processes
2. Moderately permeable
   - Quartz-sandstone rocks of the Numidian Flysch, characterized by primary permeability and enhanced by moderate fracturing. The morphostructural setting of the outcrops favours infiltration. The presence of springs with flow rates of 10–20 l/s highlights the existence of very large aquifers
   - Lens-shaped carbonate breccias embedded in the Numidian Flysch. Because they may give rise to the formation of small aquifers, they are not considered here in the total water budget. However, their occurrence does allow the geochemical characterization of the groundwaters in them
3. Slightly permeable or impermeable
   - Mainly clays that belong to several geological units, and that make up an impermeable threshold give rise to springs located at contacts with more permeable rocks. They are also found at the bottom of small gullies, where they allow the development of a surface-water network

Climatic framework

The climate of the area is of Mediterranean type, with mild and relatively rainy winters, and hot summers with little rain.
Available thermometric data are rather limited, as there are only four stations operating in the Madonie area: Caltanissetta, Enna, Petralia and Gangi. The average monthly temperature shows maximum values in August (24.5 °C) and minimum values in January (8.3 °C; the mean annual value is 15.6 °C).
Meteoric contributions were evaluated from the rainfall data published by the Servizio Idrografico del Genio Civile (Civil Engineers' Hydrographic Service 1990) relative to the stations inside the study area, at altitudes between 500 and 1000 m above sea level (a.s.l.). However, there is a large gap in the information about the higher areas of the basin, with consequent under-estimation of the total amount of atmospheric precipitation. In order to calculate high-altitude precipitation, a rain and snow gauge station was installed near Piano della Battaglia (1600 m a.s.l.).
Data processed for the period 1921–1990 show that maximum rainfall occurs at Petralia (823 mm/year) and the minimum at S. Caterina Villarmosa (604 mm/year). The Piano della Battaglia station registered a total precipitation of 1224 mm during the study period.

Hydrogeological water budget

Water availability was evaluated by calculating the hydrological water budget of the basin. Tributaries with vary-

ing hydrogeological characteristics (Coltro and Ferrara 1975) and the position of the hydrometric stations allowed the basin to be divided into two sub-basins. The first, represented by the Salso River strict sensu, has a surface extension of 202 km^2 and is mainly made up of impermeable rocks. The permeable portion, to the north covers $\sim$40 km^2. It does not bring much water to the basin because the groundwaters run off towards the north, thus feeding the aquifers of the River Pollina basin. The hydrogeological watershed therefore reduces the basin to 162 km^2. The second sub-basin, that of the southern Imera River, has an extension of 375 km^2 and has a hydrogeological watershed that includes the northern portion of Monte San Salvatore. The hydrogeological water budget of the entire basin was estimated by calculating meteoric contribution (P) losses caused by evapotranspiration (E), surface runoff (R) and effective infiltration (I), by means of the following equation:

$$P = R + I + E \quad (1)$$

Meteoric contributions were calculated using the average precipitation data for 1951–1990. Based on the method of Thiessen (1911), the two hydrogeological basins were subdivided into polygons, each representing the catchment areas of the rain gauge stations of Petralia, Gangi, Resuttano, Alimena, Villadoro, Villapriolo and S. Caterina Villarmosa. The average monthly rainfall was 684 mm. The average monthly temperatures were obtained from recordings at the Petralia, Enna and Caltanissetta stations during the period 1951–1970.

Evapotranspiration was estimated by means of two methods: Turc (1955), modified by Santoro (1970), and Hargreaves (1994).

The first method gives an estimate of annual evapotranspiration according to precipitation and temperature, whereas Hargreaves' equation estimates potential monthly evapotranspiration based on mean monthly temperature. By using the Hargreaves method, the calculation of annual evapotranspiration volumes was carried out considering evapotranspiration to be equal to precipitation in the months in which E>P.

For both sub-basins, the resulting estimates indicated mean annual evapotranspiration of 438 mm (Turc 1955) and 442 mm (Hargreaves 1994) respectively, which is equal to $\sim$65% of the precipitation.

By using the mean values from 1971 to 1990 from the hydrometric stations at Ponte 3 Archi (Salso River) and Ponte 5 Archi (Imera River) surface runoff coefficients were calculated and had values of 0.15 and 0.19 respectively.

Infiltration values were 20% of the precipitation (136 mm) for the Salso basin, which corresponds to $\sim$0.7 m^3/s, and 15% (102 mm), or $\sim$1.2 m^3/s, for the Imera basin. For the entire basin, water availability was assessed at slightly less than2 m^3/s.

However, the above estimates appear to exaggerate the real value of effective infiltration because of the role played by the water table beneath the river-bed, inside the cover of alluvial deposits. This is confirmed by the presence of alternating dry stretches and other areas in which water flows along the riverbed during periods of drought.

Analytical methods

Water temperature, pH and HCO_3^- contents were measured directly in the field; HCO_3^- was determined by titration with 0.1 N HCl. Water samples were filtered by means of cellulose filters (0.45 μm) and the major and minor constituents determined by Dionex 2000i ion chromatograph (reproducibility within $\pm$2%). A Dionex CS-12 column was used for determining the cations (Li, Na, K, Mg, Ca), and a Dionex AS4A-SC column was used for the anions (F, Cl, NO_3, SO_4) (Sortino and others 1991). D/H water measurements were carried out using the Kendall and Coplen (1985) technique (reaction with zinc at 450 °C), whereas $^{18}O/^{16}O$ measurements were carried out by the CO_2-water equilibration technique (Epstein and Mayeda 1953). Mass-spectrometer analyses were carried out with a Finnigan Mat 250 mass spectrometer and the results reported in δ per mil units versus V-SMOW standard. The standard deviations of the measurements are approximately $\pm$1 and $\pm$0.2‰ respectively, for the D/H and the $^{18}O/^{16}O$ measurements.

Water geochemistry

Groundwater

The southern aquifers of the Madonie Mountains feed a series of springs within the basin of the southern Imera River and Salso River. In particular, the areas in question are the southeastern flank of Monte San Salvatore and the southern flank of Pizzo Catarineci.

Among the springs in this area, two were chosen as being geochemically representative. The Cateratti spring was chosen from the Monte San Salvatore complex, and the Mandarini spring from Monte Catarineci. For comparison, the Calabrò spring was also occasionally sampled: this spring represents the carbonate characteristic of the Madonie area, although it feeds the river Pollina sited to the north of the study area.

A preliminary characterization, carried out using the Langelier-Ludwig diagram (1942; Fig. 2), shows the different geochemistry of the sampled groundwaters. Cateratti and Calabrò springs have earth-alkaline bicarbonate water, whereas the Mandarini spring has earth-alkaline chlorine-sulphate water. The Mandarini spring has lower salinity than the Cateratti and Calabrò springs.

Water chemistry is related to the different rocks and their interaction with water: the Mandarini spring is representative of the quartz-sandstone groundwaters hosted in the Numidian Flysch of Monte Catarineci. The Cateratti spring is fed by an aquifer originating in lens-shaped carbonate breccias inside the quartz-sandstone sequence. This carbonate component prevails in the chemical characterization of these waters.

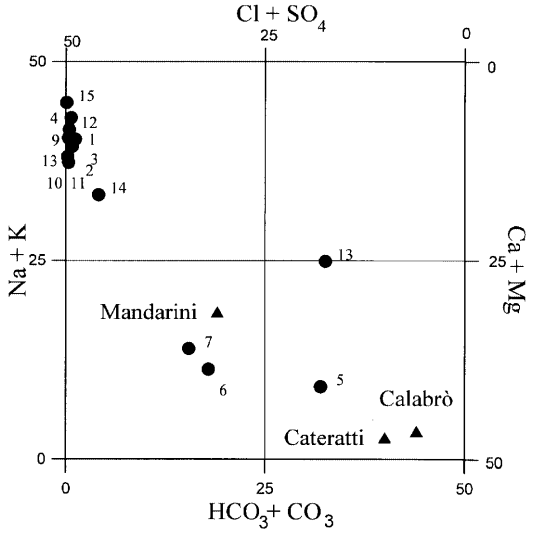

Fig. 2
Langelier-Ludwig classification diagram. The *circles* indicate the surface waters and the *triangles* represent the sampled springs

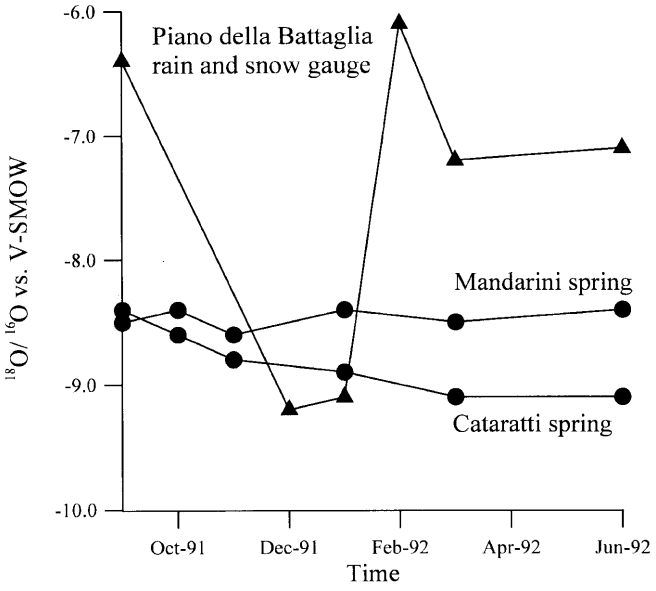

Fig. 3
$\delta^{18}O$ composition of rain and spring waters. The fluctuations in the isotopic values of the Cataratti and Mandarini springs *Closed circles* vary with respect to those of the meteoric precipitation; *open circles* collected from Piano della Battaglia rain and snow gauges

The difference in altitude between the catchment basin and the emergence points, together with the geochemical parameters, define the hydrological features of these aquifers. In both cases, these differences are quite small, but the long-term observation of chemical and isotopic data from the Cateratti and Mandarini springs reveals the different hydrological characteristics of their respective aquifers. The Mandarini spring waters have an almost constant chemical and isotopic composition throughout the hydrological year, thus indicating an extensive aquifer with a low discharge rate, which moderates seasonal variations. In contrast, the Cateratti spring has seasonal variations in both chemical and isotopic composition. In this case, the aquifer is less extensive and has a greater flow rate. However, these fluctuations in isotopic composition are modulated with respect to those of precipitation (Fig. 3), probably not only because of the characteristics of the aquifer but also because ~80% of the precipitation feeding these groundwaters occurs between November and February. In these months snow and rain show limited isotopic variations compared with those of the entire year.

The isotopic determination of $\delta^{18}O$ and δD values of both precipitation and springs shows the relationship between precipitation and groundwater and, from this, the possible catchment areas for the Cateratti and Mandarini springs can be identified.

The mean isotopic composition values of the Cateratti spring ($\delta^{18}O = -8.9\%$) are more negative than those of the Piano della Battaglia station ($\delta^{18}O = -8.4\%$). The areas involved in the recharge of the Cateratti spring are characterized by a more negative isotopic composition of the precipitation. This is probably mainly caused by three factors:

1. An altitude affect, because the catchment areas of the Cateratti spring are higher than Piano della Battaglia
2. A continental effect because the recharge areas are at the south of Piano della Battaglia
3. Precipitation in the form of snow has a great influence

Considering that the vertical isotopic gradient in the Madonie area for ^{18}O has been estimated at 0.2% δ/100 m (Hauser and others 1980), the recharge area of the Cateratti spring lies in the relief of Monte San Salvatore (1912 m a.s.l.).

The mean isotopic composition of the Mandarini spring ($\delta^{18}O = -8.5\%$) indicates a recharge area with a mean altitude of ~1600 m a.s.l. Its position and the chemical and the isotopic composition identify its most probable recharge areas to be at the top of Pizzo Catarineci

Surface waters

During a hydrologic year, 25 points along the two rivers were sampled. The inaccessibility of some sites during flood periods and the lack of runoff in many stretches during summer do not allow a complete picture of the sampling sites. However, it is possible to determine not only the precipitation regime of the areas, but also the water-rock interaction processes that influence the chemical evolution of surface waters. In particular, during winter, all sampling points show minimum concentration values because of abundant rainfall, whereas in summer little precipitation and high temperatures favour evaporation, which generates hypersaline waters in some stretches of the Salso River.

The space-time chemical evolution of the two main branches of the river (southern Imera River and Salso River strict sensu) and the stretch after their confluence are described below.

Southern Imera River

This name is given to the stretch of river between Portella Mandarini (station 5) and its confluence (station 2) with the Salso River strict sensu (Fig. 1).
Because of interaction processes with rocks of different composition, the waters show a chemical evolution that can be subdivided into three hydrogeochemical facies.
In the first stretch, between Portella Mandarini (station 5) and the town of Petralia Sottana (station 19), the earth-alkaline bicarbonate waters have a $Ca+Mg:HCO_3$ ratio close to one. Their salt contents are low, reaching 185 mg/l in flood periods (Fig. 4). These headwaters seem to be the result of the mixing of a Mandarini-type water and a Cateratti-type water (Fig. 3). The lithological substrate on which this stretch of the river flows is characterized by the presence of Portella Mandarini clays. These surface waters reflect the chemical composition of the groundwaters hosted in the Madonie reliefs.
In the second stretch, between stations 19 and 18, there is a progressive increase in salt contents, with total dissolved solid (TDS) values reaching 2000 mg/l during summer (station 18). In particular, the river crosses the gypsum outcrops, thus causing a gradual increase in Ca and SO_4 content. Further downstream, the river waters are diluted by contributions from the seasonal Alberi San Giorgio stream. Near the point of confluence a slight increase in Na and Cl content can be noted.
The third stretch, between station 18 and the point immediately before the confluence of the Vaccarizzo stream (station 14), shows a clear increase in the concentrations of all major elements, with the exception of bicarbonate. This last portion of the river crosses evaporite rocks that are mainly composed of sulphate and chloride salts, thus causing increases in Ca, SO_4, Na and Cl^-. In February, TDS values at station 14 reached 27 g/l.
Waters from the Vaccarizzo stream enter immediately after station 14 and before confluence between the southern Imera and the Salso Rivers (station 2). This seasonal stream has very high salinity values because it passes through outcroppings of salty clay and layers of halite. Salt content, caused almost entirely by the presence of NaCl, does not fall below 16 g/l during the rainy season, and can reach 250 g/l during periods of drought.
Although the mean flow rate of the Vaccarizzo stream is very low during the year, its high salt load influences the chemistry of the southern Imera River.

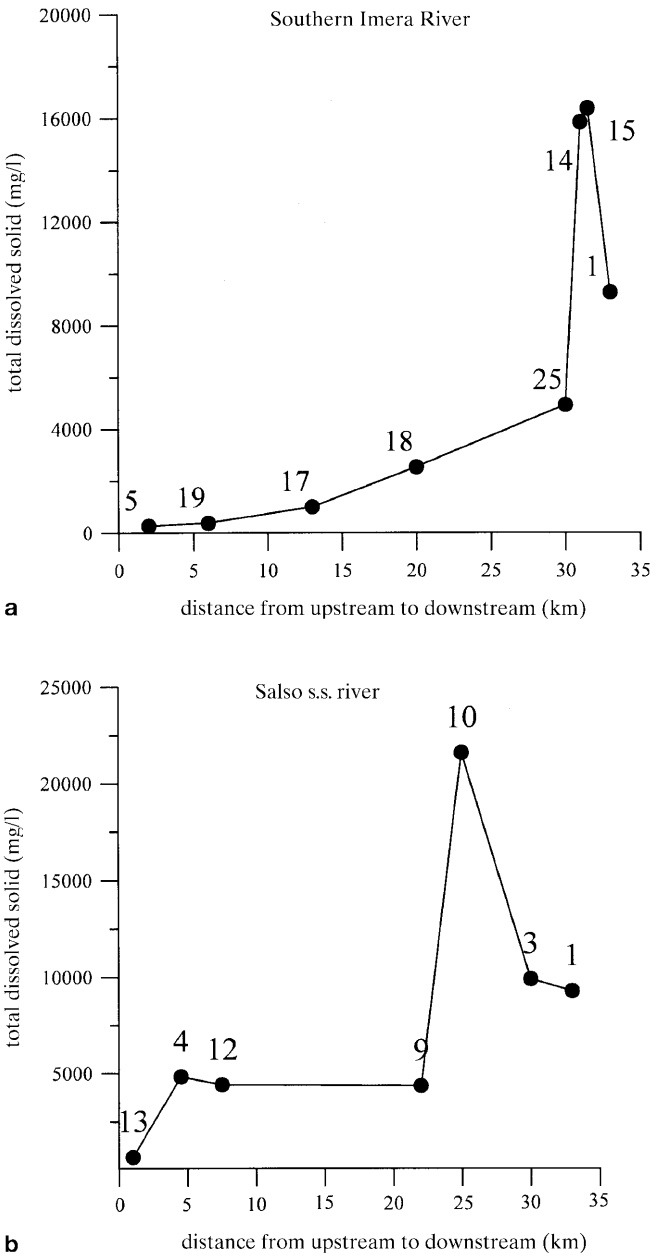

Fig. 4
Variation of total dissolved solids (TDS) along the flow path direction relative to the **a** southern Imera River and **b** the Salso River strict sensu in February

Salso River strict sensu

The stretch of the Salso River strict sensu considered here extends between Portella Bifolchi (station 13) and the confluence with the Imera River (station 3). The contribution of the seasonal streams (Salito and Corvillo) is important in determining the chemical composition of the Salso River, and their chemistry is very similar to that of Vaccarizzo water, although salinity is lower.
Increases in the major elements are related to interactions between the waters of the Salso River strict sensu and the surrounding lithotypes; however, there are some variations that, within the general evolutionary picture, appear to be anomalous (Fig. 4b).
The headwaters of the Salso strict sensu waters are represented by station 13, where the water has higher salinity (TDS = 700 mg/l) than that of the Mandarini spring, fed by the Monte Catarineci aquifer (Fig. 2). This difference is caused by a relative increase in HCO_3 with respect to Cl and SO_4, probably as a result of the presence of carbonate lens-shaped bodies embedded within the Wild Flysch outcrop at Portella Bifolchi.

The second sampling point (station 4) is immediately downstream from a salt mine. The overall chemical data show that the increased content of Na and Cl in the water is not always correlated with the flow rate of the river. This increase, in this short stretch of about 4 km, seems to indicate that the river water interacts with layers of halite. This is not supported by geological data, because this part of the river crosses the coloured clays and marls of the Polizzi Formation. The increased salinity at this point therefore appears to be caused by the discharge of waste products from the mine. Presumably, this discharge is not continuous throughout the year because, unlike all the other sampling points, there is no correlation between flow rate and Na and Cl contents. In fact, when river flow is not high (Q = 34 l/s), the Na concentration is 327 mg/l, whereas, when flow is higher (Q = 56 l/s), Na values may reach 2885 mg/l.

Station 12 is ~3 km downstream from station 4 and shows some anomalous characteristics, mainly in temperature. Analysis of the thermal profile of the Salso River strict sensu in October and March (Fig. 5) shows that station 12 water undergoes heating of between 3 and 5 °C. This is not caused by solar heating of surface waters because the increase in temperature is also recorded during winter months, when the air temperature is far lower than that of the water. In addition, it was observed that, when flow rate is high, salt concentrations at stations 4 and 12 are more or less the same, whereas in July and August the salt load of station 12 is about half that of station 4 (Table 1). This anomaly may be caused by the entry of low-salinity thermal water into the river, which is chemically similar to the water circuit in the quartz-sandstone of Pizzo Catarineci (Mandarini-type waters). A term with these characteristics would explain both the heating and the water dilution.

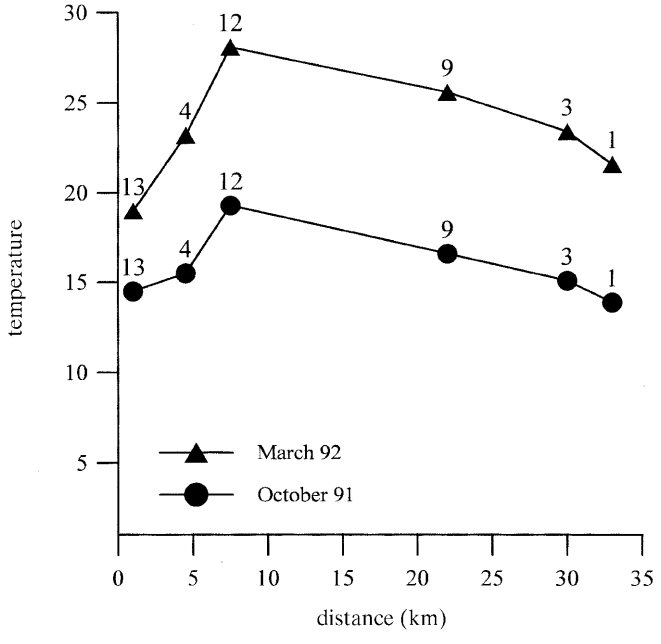

Fig. 5
Thermal profile of the Salso River strict sensu. Downstream from station 4 it is possible to see the increase in temperature caused by the mixing between surface and thermal waters

By comparing the chemical data of stations 12 and 16, it is clear that the water of the Gangi River greatly influences the Salso River strict sensu. According to the presence or absence of waste discharge from the salt mine, the Gangi River tends either to dilute or concentrate the waters of the Salso River strict sensu. As already observed for the southern Imera River, in the stretch between stations 9 and 3, a considerable increase in salinity, may be caused by waters from the Salito (station 10) and Corvillo streams, with high salt contents.

Station 1 constitutes the final part in the chemical evolution of the Salso and southern Imera Rivers. The data from stations 1, 2 and 3 reveal that the chemical features of these waters are closely correlated with river capacity and thus with the climatic regime of the area.

During the rainy season, station 1 waters have intermediate chemical characteristics between those of stations 2 and 3, and is closer to those of the Imera River, because of the greater flow of the Imera River with respect to the Salso River strict sensu.

The salt content in May at station 1 is higher than at the stations 2 and 3, and this is probably caused by evaporation processes enhanced by high temperatures (>20 °C between June and September) and low flow rate. This hypothesis is confirmed by the strongly positive isotopic values of station 1 waters with respect to those of stations 2 and 3. The δD versus δ^{18}O diagram in Fig. 6 shows that almost all the points of surface waters plot inside the Mediterranean Meteoric Water Line (MMWL) (Gat and Carmi 1970) and the Meteoric Water Line (MWL) (Craig 1961), thus confirming a meteoric origin. Exceptions are station 1 samples in May and June, which have more positive values along an evaporation curve.

The chemical evolution of the two river branches is shown in the modified Langelier–Ludwig diagram (Fig. 7) in which SO_4^{2-} ion species were combined together with HCO_3^- and CO_3^{2-}.

The surface water body shows an inverse correlation between river flow rate and salt content (Fig. 8). As expected, in the rainy season, the great quantities of meteoric water dilute the surface waters. In addition, the interaction times between surface waters and outcropping rocks is limited, which results in minimum salt concentrations. Conversely, during periods of drought, low rainfall, low flow rates and high temperatures all combine to favour the evaporation of waters, which reach peak salinity in August. Isotopic composition values also indicate evaporation processes during summer.

Water quality and anthropogenic action

One of the aims of this study was to define the surface water quality for drinking use and irrigation purposes.

Table 1
Physico-chemical data and isotopic composition of surface waters. Concentrations are expressed in mg/l (±2%). Temperature (T) is expressed in °C (±0.1 °C), pH in pH units (±0.01), conductivity in μS/cm (±5%) at 25 °C. *SAR* sodium absorption ratio. The isotopic compositions of oxygen and hydrogen are reported in δ unit per mil versus V-SMOW standard. (D/H ± 1‰ and $^{18}O/^{16}O = \pm 0.2‰$)

Site	Date	T	pH	Cond.	Na	K	Ca	Mg	Cl	HCO_3	SO_4	NO_3	TDS	$\delta^{18}O$	δD	SAR
1	09.91	20.1	7.35	–	10623	535	1289	855	18445	125	4186	–	36057	–	–	325
	10.91	13.9	8.30	23338	3792	340	409	329	6494	214	1584	–	13162	−5.7	−36	197
	11.91	6.4	–	17426	2636	184	386	225	4438	214	1166	–	9249	−6.1	−37	151
	12.91	5.7	8.12	2701	294	17	172	34	416	214	379	–	1526	–	–	29
	02.92	–	8.11	–	2634	129	295	371	4030	244	1550	18	9270	−5.9	−35	144
	03.92	12.6	7.93	23075	3250	243	600	369	5346	198	2102	–	12108	−5.0	−31	148
	04.92	15.1	8.31	9146	1594	83	244	127	2620	198	912	–	5779	−6.3	−38	117
	05.92	21.6	–	–	5542	495	1176	590	9509	153	3715	–	21181	−1.4	−16	186
	06.92	22.2	8.15	46940	8684	1029	822	678	14106	165	3653	–	29136	−2.8	−21	317
	07.92	24.9	8.18	–	10502	547	1100	693	16509	122	4200	–	33672	–	–	351
	08.92	–	–	–	12245	782	1317	940	21245	116	4579	–	41224	–	–	364
2	09.91	23.0	7.54	–	36219	3575	927	2110	58283	235	9998	–	111348	–	–	929
	10.91	13.9	8.09	18513	3011	280	318	217	4995	244	1203	–	10268	–	–	184
	05.92	22.3	–	–	4145	338	395	314	6658	183	1690	–	13722	–	–	220
	06.92	23.3	8.30	965	16646	112	669	1143	25570	183	4934	–	49258	–	–	553
3	09.91	23.3	7.54	–	9041	451	1194	840	15226	183	3979	–	30914	–	–	284
	10.91	15.1	8.46	44798	8496	507	1053	832	14790	122	3706	–	29505	–	–	277
	11.91	7.8	–	23014	2988	158	591	288	5299	153	1520	–	10997	–	–	143
	02.92	–	8.33	–	3073	106	323	188	4396	214	1589	–	9888	–	–	192
	03.92	13.0	7.94	25878	3288	146	597	379	5201	171	2366	–	12148	–	–	149
	04.92	15.6	8.30	10118	1747	55	304	135	2811	195	1050	–	6297	–	–	118
	05.92	23.4	–	–	2901	196	547	230	4538	174	1704	–	10289	–	–	147
4	09.91	20.9	7.47	–	7969	20	731	125	12532	153	1339	–	22869	–	–	385
	10.91	15.5	8.30	23217	4166	12	463	87	6615	168	1024	–	12535	−6.7	−38	251
	11.91	9.5	–	8591	1374	9	203	43	1999	244	511	–	4382	−6.5	−35	124
	12.91	7.8	8.48	1182	104	5	105	17	146	183	198	–	759	–	–	13
	02.92	–	8.48	–	1631	6	139	17	2301	186	547	4	4827	−7.3	−44	185
	03.92	11.8	8.10	19206	2895	9	338	60	4428	220	933	–	8882	−6.8	−41	205
	04.92	16.2	8.87	2367	327	6	160	28	425	204	413	–	1563	−7.4	−43	34
	05.92	23.2	–	–	3057	9	343	61	4523	183	1003	–	9179	−7.0	−42	215
	06.92	20.8	8.20	29815	7076	18	475	86	10784	214	1411	–	20064	−6.5	−41	422
	07.92	24.2	8.08	–	7507	16	739	112	11408	204	1675	–	21661	–	–	364
	08.92	–	–	–	9343	19	874	134	14570	183	1786	–	26908	–	–	416
5	09.91	14.6	7.84	191	14	2	21	7	11	92	22	–	168	–	–	4
	10.91	10.6	8.00	309	10	1	31	7	13	98	26	–	186	–	–	2
	11.91	6.8	–	249	10	1	23	6	13	70	25	–	149	–	–	3
	12.91	5.1	7.85	221	10	2	17	4	21	40	17	–	111	–	–	3
	02.92	–	7.92	196	121	2	20	3	18	85	21	2	270	–	–	3
6	09.91	21.3	7.91	914	102	16	86	32	71	183	311	–	802	–	–	13
	10.91	12.2	8.42	1272	52	10	124	31	67	244	254	–	781	−7.2	−43	6
	11.91	12.8	–	1047	52	9	105	27	55	198	221	–	668	−7.3	−42	6
	12.91	7.4	8.42	829	38	5	83	19	43	183	144	–	515	–	–	5
7	09.91	22.2	7.78	1059	87	15	135	35	77	214	367	–	929	–	–	9
	10.91	13.1	8.64	1479	79	10	130	38	77	244	327	–	904	–	–	9
8	09.91	19.6	7.53	5044	548	13	636	196	920	153	1959	–	4425	–	–	27
9	10.91	16.6	8.29	26059	4536	43	661	178	7747	92	1238	–	14496	−4.8	−29	222
	11.91	8.1	–	11513	1745	21	337	92	2776	198	720	–	5889	−6.1	−35	119
	12.91	8.1	8.47	2253	223	10	170	26	355	229	277	–	1289	–	–	22
	02.92	–	8.27	–	1395	14	159	29	1183	244	1315	9	4347	−6.0	−37	144
	03.92	13.0	7.97	7752	1301	20	324	89	2098	210	843	–	4885	−5.5	−29	91
	04.92	16.1	8.38	4474	663	12	175	46	979	226	505	–	2605	−6.4	−38	63
	05.92	25.6	–	–	1198	13	253	72	1822	189	732	–	4278	−5.2	−36	94
	06.92	23.6	7.97	11693	2233	40	421	116	3375	180	1104	–	7468	−4.7	−31	136
10	10.91	17.7	8.73	35773	6652	188	1132	538	11241	153	2957	–	22861	–	–	230
	02.92	–	8.11	–	6212	177	1084	541	10595	147	2859	11	21615	–	–	–
11	10.91	21.5	8.90	21630	3852	176	827	430	6342	137	2918	–	14684	–	–	154

Table 1
Continuous

Site	Date	T	pH	Cond.	Na	K	Ca	Mg	Cl	HCO_3	SO_4	NO_3	TDS	$\delta^{18}O$	δD	SAR
12	10.91	19.3	9.19	20077	3498	22	488	90	5647	92	940	–	10777	−6.1	−35	206
	11.91	12.4	–	10714	163	14	224	54	262	168	562	–	1446	−6.5	−36	14
	12.91	8.4	8.60	416	243	7	157	20	400	214	240	–	1280	–	–	26
	02.92	–	8.81	–	1454	9	137	18	2041	171	562	6	4397	−7.2	−41	165
	03.92	17.3	8.36	15915	3149	14	328	62	4881	198	869	–	9501	−6.6	−39	226
	04.92	19.0	8.78	3295	506	8	167	11	744	128	447	–	2011	−7.2	−42	54
	05.92	28.1	–	–	2519	11	269	53	3722	174	720	–	7468	−6.6	−39	199
	06.92	24.8	8.55	17357	4175	11	401	79	6232	146	974	–	12018	−6.1	−36	270
	07.92	26.9	8.18	–	4138	23	501	88	6264	183	1229	–	12426	–	–	241
	08.92	–	–	–	4374	26	461	102	6675	137	1032	–	12807	–	–	261
13	10.91	14.5	8.13	1021	104	4	67	16	25	366	120	–	703	–	–	16
	02.92	–	8.17	–	112	3	61	15	34	335	127	–	687	–	–	15
	05.92	19.0	–	–	121	3	58	14	52	305	138	–	692	–	–	20
14	10.91	14.3	8.25	4567	668	29	171	79	962	214	587	–	2710	–	–	60
	11.91	7.9	–	3850	391	20	199	59	645	244	446	–	2004	–	–	34
	12.91	7.3	7.23	1756	128	12	108	29	189	214	243	–	922	–	–	16
	02.92	–	8.43	–	4695	496	377	265	7135	229	2611	–	15807	–	–	262
15	10.91	17.9	7.70	47423	47724	5235	786	2650	82988	259	12436	–	152078	–	–	1151
	11.91	10.1	–	1666	28304	2063	786	1373	43845	244	7502	–	84117	–	–	861
	12.91	8.7	8.48	43646	7562	646	692	527	12767	259	2786	–	25240	–	–	306
	02.92	–	8.45	–	4951	453	383	362	7445	238	2502	–	16333	–	–	256
	03.92	13.2	8.40	63730	11411	940	627	706	18622	207	4061	–	36575	–	–	442
	04.92	17.5	8.49	54600	11141	895	645	676	18633	189	3920	–	36099	–	–	433
	05.92	22.8	–	–	23381	2358	886	1386	36609	207	7171	–	71999	–	–	694
	06.92	22.4	7.80	50570	56313	4429	1417	3236	90096	259	15134	–	170884	–	–	1168
	07.92	26.6	7.59	–	79875	7062	972	3941	124461	278	21206	–	237796	–	–	1612
	08.92	–	–	–	75914	6081	839	3070	117382	244	15581	–	219110	–	–	1717
16	02.92	10.1	–	15215	2498	33	417	117	4038	259	936	–	8298	–	–	153
	05.92	25.3	–	–	774	78	283	68	1212	174	748	–	3337	–	–	58
17	02.92	–	8.35	–	168	12	72	29	93	305	297	26	1001	–	–	24
18	02.92	–	7.99	–	609	19	124	80	842	275	576	12	2537	–	–	60
	03.92	12.0	7.70	6264	689	27	173	101	1074	238	581	–	2883	–	–	59
	04.92	14.9	8.01	1675	190	10	109	38	272	201	289	–	1109	–	–	22
	05.92	21.2	–	–	650	47	202	74	1003	229	543	–	2749	–	–	55
	06.92	18.8	8.10	9728	1700	35	285	180	2804	220	814	–	6037	–	–	112
19	02.92	–	8.02	–	43	3	41	12	17	159	99	9	382	–	–	8
	03.92	10.7	8.45	480	23	4	62	17	19	171	106	–	402	–	–	4
	04.92	13.1	8.30	503	20	3	50	13	16	128	86	–	316	–	–	4
	05.92	15.8	–	–	21	2	54	15	16	146	91	–	345	–	–	4
	06.92	14.9	8.40	584	37	8	64	18	21	183	102	–	433	–	–	6
	07.92	19.4	8.23	–	34	8	86	24	34	244	125	–	555	–	–	5
	08.92	–	–	–	30	9	64	17	33	153	116	–	421	–	–	5
22	02.92	–	8.30	–	139	12	93	30	97	275	304	479	1429	–	–	18
23	02.92	–	7.95	–	109	14	56	13	78	244	132	1	647	–	–	19
	03.92	16.9	7.95	1104	76	12	96	20	75	275	149	–	702	–	–	10
24	04.92	15.2	8.75	638	29	4	71	17	27	275	149	–	571	–	–	4
25	02.92	–	8.28	–	1298	40	204	185	1926	244	1013	11	4921	–	–	93
	03.92	12.6	8.11	10676	1248	53	311	190	2278	223	984	–	5286	–	–	79
	04.92	15.9	8.32	3462	394	30	145	68	594	189	443	–	1864	–	–	38
	05.92	20.5	–	–	1276	92	289	168	2095	189	960	–	5068	–	–	84
	06.92	18.3	8.00	19853	3247	160	563	443	5392	183	2090	–	12078	–	–	145

The presence of towns, human activities such as agriculture, animal breeding and farming, and quarrying all exert anthropogenic pressure on the quality of surface water and groundwaters in the basin.

In order to evaluate the level of pollution, on the basis of a February sampling, a graph representing the spatial distribution of NO_3 concentrations in the basin was made (Fig. 9). Nitrate is the most common form of nitrogen that occurs in surface water and groundwater (Kacaroglu and Gunay 1997). Because of its anionic form, nitrate is very soluble and mobile in aqueous solution. It represents the oxidized end product in the nitrogen cycle of atmosphere, vegetation, upper soil and soil water zones. Concentrations of NO_3^- are the result of different pollu-

Table 2. Physico–chemical data of sampled springs. Concentrations are expressed in mg/l (±2%). Temperature (T) is expressed in °C (±0.1 °C), pH in pH units (±0.01), conductivity in μS/cm (±5%) at 25 °C. *SAR* Sodium absorption ratio

Sample	Date	T	pH	Cond.	Na	K	Ca	Mg	Cl	HCO_3	SO_4	TDS	SAR
Cateratti	09.91	9.0	7.40	561	6	<1	57	25	7	232	37	363	1
	10.91	9.7	–	519	6	1	57	24	7	235	37	367	1
	11.91	10.1	–	515	6	2	57	25	6	238	36	370	1
	01.92	5.2	7.50	518	5	2	56	26	7	238	38	372	1
	03.92	8.5	7.59	469	6	<1	56	24	9	220	38	352	1
	06.92	11.8	–	482	5	<1	55	24	7	229	37	357	1
Mandarini	09.91	13.1	6.34	205	13	<1	15	4	15	34	27	107	4
	10.91	11.7	–	187	13	<1	14	4	15	37	27	109	4
	11.91	10.7	–	213	13	<1	15	4	15	37	29	113	4
	01.92	9.6	6.56	184	12	<1	15	4	17	31	25	104	4
	03.92	8.6	6.06	162	13	<1	11	3	16	27	22	92	5
	06.92	11.8	6.39	192	14	2	14	3	17	34	26	111	5

tion processes: (1) municipal wastewaters and (2) fertiliser and pesticide application in agriculture. The highest concentration, recorded at station 22, was mainly caused by the position of the sampling station itself, which was downstream from the point at which the town of Gangi wastewater was discharged. Discharge of polluting substances means that the waters of this entire river branch, until confluence with the Salso River, cannot be used for any anthropogenic purpose, and this is particularly so when meteoric contributions are low. In the remaining portions of the basin, NO_3^- contents are more or less constant, (<40 mg/l). These values are below the standard maximum permissible limit for drinking water (nitrate<50 mg/l), as recommended by the World Health Organization (WHO 1993). However, within the studied watercourses, only the higher stretches of the southern Imera River (before station 19) have conductivity values below the maximum permissible limit for drinking water. In order to identify the availability of surface waters for irrigation use, the Wilcox classification diagram (1955) in Fig. 10 has been used. This graph is based on the electrical conductivity (EC) and on the sodium absorption ratio (SAR). This parameter is of particular importance because high Na contents in irrigation waters may increase soil hardness and reduce its permeability (Tijani 1994). The use of saline waters in permeable rocks may also in-

Table 3. Isotopic composition of sampled springs and rainwaters. Values are reported in δ unit per mil versus V−SMOW standard (D/H ± 1‰ and $^{18}O/^{16}O = \pm 0.2‰$)

Sample	Date	$\delta^{18}O$	δD
Cateratti	09.91	−8.4	−50
	10.91	−8.6	−50
	11.91	−8.8	−51
	01.92	−8.9	−51
	03.92	−9.1	−53
	06.92	−9.1	−52
Mandarini	09.91	−8.5	−47
	10.91	−8.4	−48
	11.91	−8.6	−49
	01.92	−8.4	−48
	03.92	−8.5	−49
	06.92	−8.4	−49
P. della Battaglia	09.91	−6.4	−29
	12.91	−9.2	−53
	01.92	−9.1	−51
	02.92	−6.1	−28
	03.92	−7.2	−37
	06.92	−7.1	−42

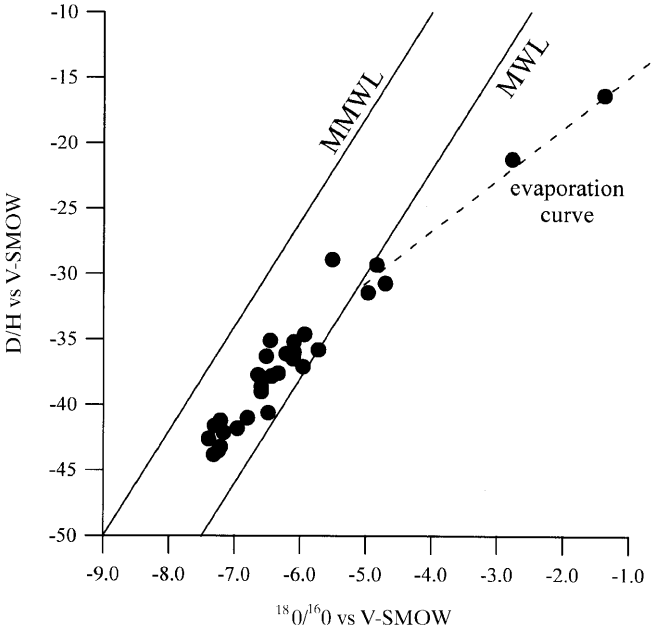

Fig. 6
δD-$\delta^{18}O$ diagram. Almost all the samples lie within the Meteoric Water Line (MWL) (Craig 1961) and the Mediterranean Meteoric Water Line (MMWL) (Gat and Carmi 1970). During the dry season, the Salso River water lies along an evaporation curve (*dashed line*), because of the low flow rate and high temperature

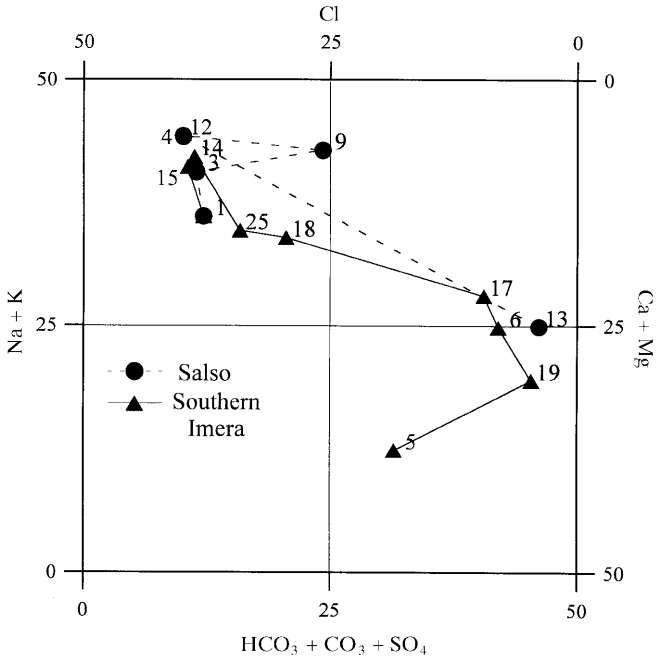

Fig. 7
Chemical evolution of the southern Imera River (*dashed line*) and Salso River strict sensu (*solid line*) in February

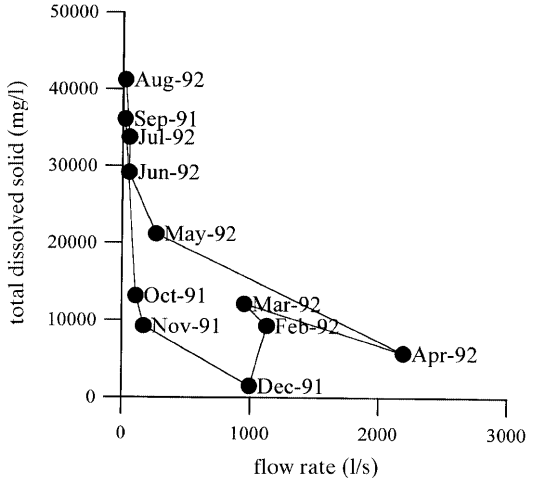

Fig. 8
Relationships between total dissolved solid and flow rate relative to station 1

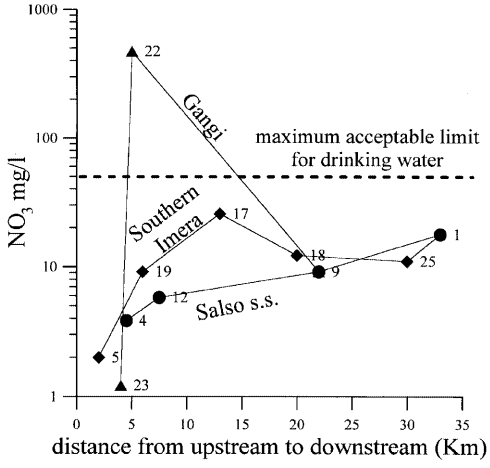

Fig. 9
Variation of NO_3 content from upstream to downstream in February. *Dashed lines* ($NO_3 = 50$ mg/l) indicate the maximum acceptable limit for drinking water (WHO 1993). As pointed out in the text, almost all the surface waters fall below the limit fixed for human consumption. The high concentration recorded at station 22 is related to the position of the sampling station, which is downstream from the discharge area of wastewater from the town of Gangi

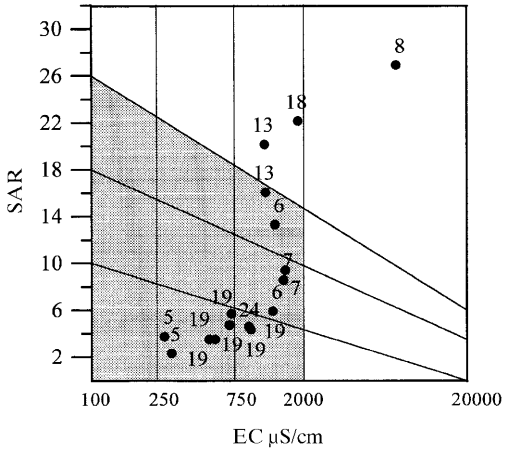

Fig. 10
Wilcox classification diagram (1955) of the surface water sampled during May–October that have EC < 20,000 µS/cm and SAR < 32. It can be seen that only a few samples are suitable for irrigation use (*dotted area*)

crease the salinity of groundwaters. In Fig. 10, the points relative to the surface waters that have SAR < 32 and EC < 20,000 µS/cm are shown relative to the May–October period when water requirements for irrigation are highest. Overall examination of the basin shows that, in this period, SAR and EC values permit only limited water use for agricultural purposes and this is restricted to only the surface waters of the southern Imera River before station 18.

Conclusion

This geochemical study of the waters of the Salso River highlights the physico-chemical processes along its flow path. Stream and river water quality is controlled by meteorological and hydrological conditions and by the geological setting of the catchment area. Chemical and isotopic observations relative to 25 points along the Salso River lead to the following conclusions:

1. Concentrations of ionic species and river flow rate are inversely correlated
2. The prevalence of one ionic species over others varies throughout. Water from the northern part of the basin have Ca^{2+} as the dominant cation and HCO_3^- as prevalent anion, whereas in central and southern parts Ca-SO_4 and Na-Cl contents respectively prevail. These variations are always accompanied by marked increases in salinity because the water crosses sediment that belongs to the 'Gessoso-Solfifera' series
3. The water in the northern stretch of the Imera River originates from the mixing of two groundwater systems: the aquifer of Monte San Salvatore (Cateratti spring type) and Pizzo Catarineci (Mandarini spring type)
4. The δD and δ^{18}O of the studied springs, together with long-term chemical observations, allow us to distinguish between the two aquifers by the following characteristics: the Mandarini spring is connected to an extensive aquifer with a low discharge rate; the Cateratti spring has a less extensive aquifer with a greater flow rate
5. Much of the salinity of the Salso River is caused by the high salinity of its tributaries (Vaccarizzo, Corvillo and Salito seasonal streams), although these streams have low flow rates with respect to those of the Salso River
6. An increase in water temperature was observed between sampling stations 4 and 12 along the course of the Salso River strict sensu. This is probably because of the addition of thermal water with low salt contents, which dilute highly concentrated waters during the summer
7. The anomalous increase in salinity of the waters of the Salso River strict sensu near the village of Raffo is caused by salt mine wastewater
8. The polluting load recorded along the Salso River is principally caused by discharges of urban wastewater, as many towns do not have a purification plant, and by periodic discharges from the salt mine
9. The chemical analyses show that only waters from the top portion of Salso River can be used for drinking water. During the period of irrigation (from June to October), the water availability that has SAR values that permits their use for agricultural purposes ($<$26 mg/l) is rather limited and restricted only to the surface waters of the southern Imera River before station 18. In the lower reaches, because of interaction with extremely soluble rocks and anthropogenic action, the water can only be utilized for drinking and irrigation use after suitable treatment

References

Catalano R, D'Argenio B (1982) Schema geologico della Sicilia. In: Guida alla geologia della Sicilia occidentale. Ed Soc Geol Ital 1. Centenario della società geologica italiana 3:102

Craig H (1961) Isotopic variation in meteoric waters. Science 133:1702–1703

Coltro R, Ferrara V (1975) Lineamenti geomorfologici del bacino del F. Salso nel quadro della sistemazione idrogeologica e della pianificazione delle acque. Proceedings 2nd International Conference on Water Resources, Palermo, 5–10 June 1975

Epstein S, Mayeda T (1953) Variation of ^{18}O content of water from natural sources. Geochim Cosmochim Acta 4:213–224

Gat JR, Carmi H (1970) Evolution of the isotopic composition of atmospheric waters in the Mediterranean Sea area. J Geophys Res 75:3039–3040

Grasso M, Lentini F, Vezzani L (1978) Lineamenti stratigrafico strutturali delle Madonie. Geol Rom 17:58–79

Hargreaves GH (1994) Defining and using reference evapotranspiration. J Irrigat Drain Eng 120:77–91

Hauser S, Dongarrà G, Favara R, Longinelli A (1980) Composizione isotopica delle pioggie in Sicilia. Riferimenti di base per studi idrogeologici e relazione con altre aree Mediterranee. Rend Soc Ital Min Petrol 36:671–680

Kacaroglu F, Gunay G (1997) Groundwater nitrate pollution in an alluvium aquifer, Eskisehir urban area and its vicinity, Turkey. Environ Geol 31:221–230

Kendall C, Coplen TB (1985) Multisample conversion of water to hydrogen by zinc for stable isotope determination. Anal Chem 57:1437–1440

Langelier WF, Ludwig HF (1942) Graphical methods for indicating the mineral character of natural waters. JAWWA 34:335

Santoro M (1970) Sull'applicabilità della formula del Turc per il calcolo della evapotraspirazione efettiva in Sicilia. Atti I Convegno Int Acque Sotterranee, Palermo, Italy

Servizio Idrografico del Genio Civile (1990) Annali idrologici. Parte I e II. Regione Siciliana Ed, Palermo

Sortino F, Inguaggiato S, Francofonte S (1991) Determination of HF, HCl, and total sulfur in fumarolic fluids by ion chromatography. Acta Vulcanol 1:89–91

Thiessen AH (1911) Precipitation average for large areas. Monthly Weather Rev 3:5–25

Tijani J (1994) Hydrochemical assessment of groundwater in Moro area, Kwara State, Nigeria. Environ Geol 24:194–202

Turc L (1955) Le bilan D'eau des sols. Relation entre les precipitations, l'evaporation et l'ecoulement. Ann Agron 5:125–144

WHO (1993) Guidelines for drinking-water quality, vol 1. Recommendations. WHO, Geneva

Wilcox LV (1955) Classification and use of irrigation waters. US Dept Agric Circ, p 969